International Journal of Innovative
Computing, Information and Control
Volume **14**, Number **3**, June **2018**

ICIC International ©2018 ISSN 1349-4198
pp. 915–928

PIXEL FILTERING AND REALLOCATION WITH HISTOGRAMS OF SECOND-ORDER DERIVATIVES OF PIXEL VALUES FOR ELECTRON MICROSCOPE IMAGES

Wai Ti Chan, Kok Swee Sim and Fazly Salleh Abas

Faculty of Engineering and Technology
Multimedia University
Jalan Ayer Keroh Lama, Bukit Beruang, Melaka 75450, Malaysia
{ wtchan; kssim; fazly.salleh.abas }@mmu.edu.my

Received October 2017; revised February 2018

Abstract. *The proposed method uses second-order derivatives to derive more information from the gray values of the pixels in a scanning electron microscope image. It represents this information as a histogram of second-order values, which expresses the variation in pixel values caused by image details and noise. The method uses the histogram as the basis for the targeting of pixels for filtering and reallocation to restore the image. The method controls the number of target pixels to minimize blurring of edges by imposing a Laplace curve on the histogram and using it together with other equations to select pixels based on the differences between their second-order derivatives and those of their neighbours.*

Keywords: Second-order derivatives, Laplace curve, Laplacian operator, Histograms, Pixel reallocation, Noise filter, SEM images

1. **Introduction.** The proposed method makes use of the effect of noise on the variation of gray values between pixels of a scanning electron microscope (SEM) image in the spatial domain. It expresses the variation of gray values between pixels with the second-order derivatives of each pixel and its neighbours. Image processing has utilized the second-order derivatives of pixels before, such as in detecting edges in images [1]; the proposed method uses them to minimize blurring. The proposed method uses the Laplacian operator to generate the second-order derivatives. Existing filtering methods have utilized the Laplacian operator in manners such as a means for image segmentation and noise removal [2]. The proposed method presents the second-order derivatives as histograms, henceforth referred to as "second-order histograms" to differentiate them from histograms of gray values. The second-order histograms, before and after noise is introduced, express changes in the distribution of the second-order values. The statistics of these histograms are used in the processing of the images [3]. Next, the method uses a Laplace curve as a target for the pixel reallocation phase, similar to the use of probability density functions to modify histograms [4]. The reallocation phase selects and categorizes pixels according to the differences between their second-order derivatives and those of neighbours, and changes their derivatives through a convolution process; this is similar to how the work of Celestre et al. defined bad pixels and corrected them [5]. The proposed method uses the changes to generate an image with reduced noise.

The proposed method utilizes several techniques, namely collation of data as histograms, histogram statistics, thresholds, convolution and pixel reallocation; this decision was made after reviews of the typical use of these techniques [3,6]. The proposed method

intends to contribute to the use of histograms in image processing by providing proof-of-concept for the use of second-order derivatives as the data in histograms, instead of the usual use of gray values and their normalized derivatives.

2. Definitions, Hypothesis, Theory and Problem Statement.

Definition 2.1. Second-order derivatives: *The proposed method applies a two-dimensional Laplacian operator on each pixel to obtaining an isotropic second-order derivative using a 3 × 3 mask [7]. For pixels that are on the edges of the image, it alters the equation and mask to accommodate the edges.*

Definition 2.2. SEM images used for testing: *The testing of the filter uses SEM images with additive noise of increasing severity. The additive noise has a Gaussian distribution of nominal zero mean and different nominal standard deviations. There are 30 original images and their 300 noise-added versions. The testing also uses SEM images with different conditions of the SEM machine such as aperture size [8], scan rates [9], acceleration voltage and chamber pressure [10]. These are 36 images of these images in total, obtained with permission from other research efforts, such as Sim et al. [9].*

Definition 2.3. PSNR, SSIM & RMS contrast: *The method calculates the PSNR ratings of the images according to the description by Salomon [11] and their SSIM ratings according to the description by Wang et al. [12]. It measures the contrast of the images in root-mean-square (RMS) contrast, as described by Peli [13].*

Definition 2.4. Laplace distribution curve: *For the example image in Figure 1(a), the method generates the histogram of second-order derivatives as shown in Figure 2, whereas it generates the histogram as shown in Figure 3 for the image in Figure 1(b). The method imposes a Laplace distribution curve onto the second-order histogram. One of the steps to generate the curve uses Equation (1), which is the Laplace probability function.*

$$f(x|\mu, b) = \frac{1}{2b} \exp\left(-\frac{|x-\mu|}{b}\right) \tag{1}$$

The diversity is $b = (\sigma/2^{0.5})$, where σ is the standard deviation of the second-order derivatives. x represents a second-order derivative value that is in the image. σ can be calculated

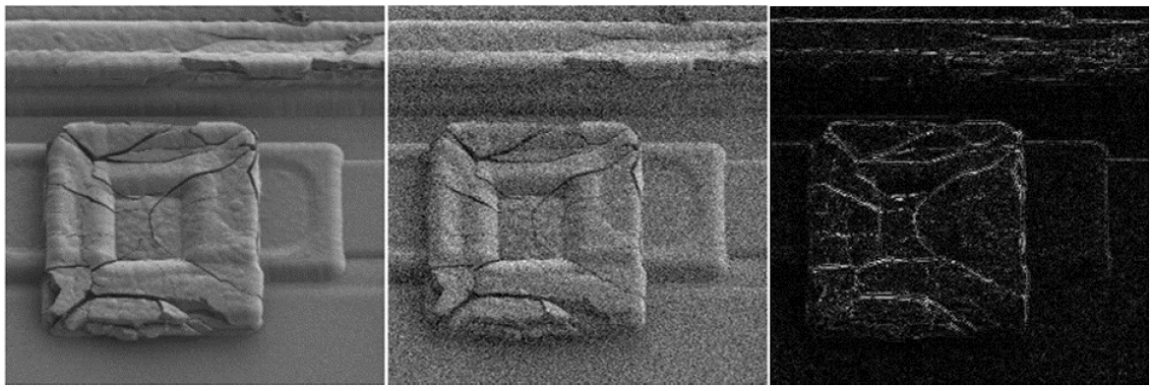

(a) (b) (c)

FIGURE 1. SEM image of a defect in an electronic element: (a) original, (b) additive noise introduced with a Gaussian distribution of zero mean and standard deviation of 20, and (c) the second-order derivatives of the image in (a), represented as a grayscale image

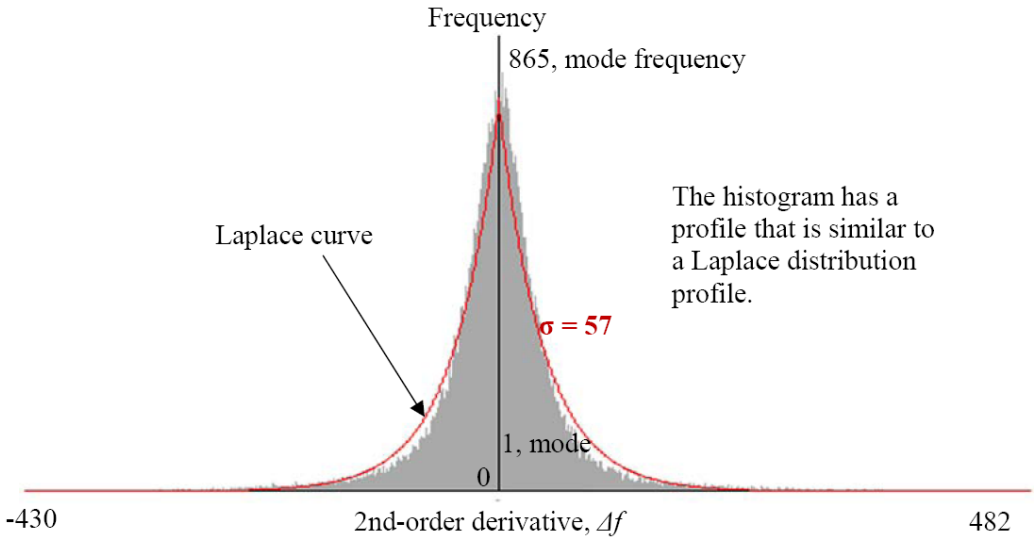

FIGURE 2. Second-order derivative histogram of image in Figure 1(a)

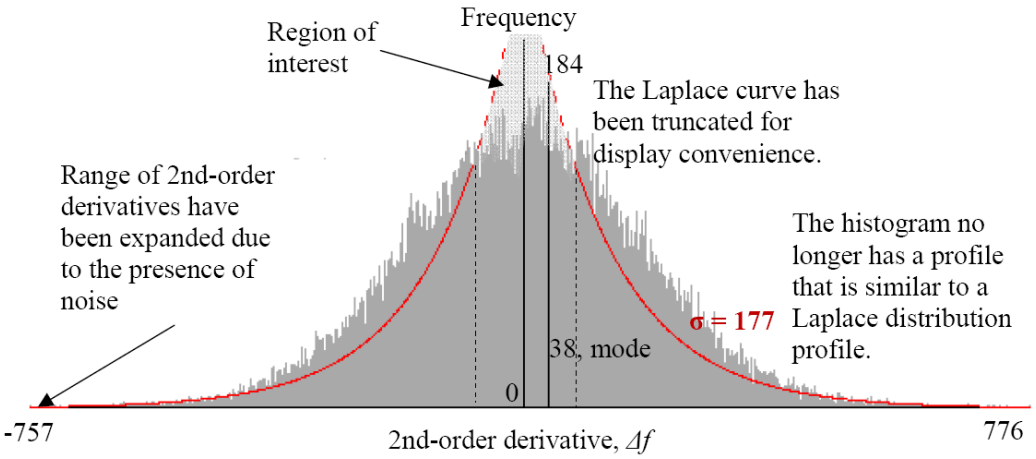

FIGURE 3. Second-order derivative histogram of image in Figure 1(b)

from the data set of the derivatives together with mean (μ). Since b is dependent on σ, the method uses σ as the representative quantity of the Laplace distribution.

The method multiplies the probability with the total number of pixels to produce a projected number of pixels for that second-order derivative value. Then, it uses the projected numbers to construct the Laplace curve.

Hypothesis 2.1. Utilization of the second-order histogram and curve. The proposed method makes use of a Laplace distribution curve on the histograms of second-order derivatives [14]. The hypothesis is that an SEM image without additive noise generates a histogram of second-order derivatives that closely follows a Laplace distribution. For an image with low noise and clear contrast, the histogram profile is close to that of the curve. For example, Figure 2 shows that the profile of the second-order histogram is close to the imposed Laplace curve. However, there is a wider range of second-order derivatives for the histogram and a higher σ for the curve in Figure 3. Thus, the distribution of the second-order has deviated away from the original distribution. There is the observation that the middle region of the histogram depresses as the severity of the noise increases, as

highlighted in Figure 3. The method utilizes this change to control the filter, as described later.

Theory 2.1. Distribution of second-order derivatives in the histogram. The middle region of the second-order histogram represents uniform visual elements, such as surfaces of the same texture. The regions beyond this and to trailing ends of the second-order histogram represent other details such as edges. This idea is similar to how the divisions of an intensity histogram represent regions of an image that are under-exposed or over-exposed [15].

Proof: Figure 1(c) shows details such as edges of objects in Figure 1(a). Therefore, the second-order histogram of the image in Figure 1(a) should contain data on its details.

Problem Statement 2.1. Change in the imposed curve due to the effect of noise. The Laplace curve which is imposed on the second-order histogram of an image has a specific standard deviation, as can be observed in Figure 2. As noise increases, its standard deviation becomes greater. To reduce the noise, the method is to alter the image such that it lowers the standard deviation. However, during the development of the method, tests have found that the standard deviations of the curves for images with excessive blurring are lower than those for images that are not. Therefore, there is Step 3.1 of the methodology, which intends to find a target standard deviation that does not result in excessive blurring.

3. **Methodology.** Appendix A shows the process flow of the methodology. The steps in the methodology are as follows.

Step 3.1. Estimation of target standard deviation. This step utilizes the area between the imposed curve and the middle region of the second-order histogram. As an example, Figure 3 highlights this area. Equation (2) expresses this area ΔA.

$$\Delta A = \sum_{i=a}^{b} (P(x) - H(x)) \tag{2}$$

where a and b are the second-order derivatives which correspond to the intersections between the second-order histogram and the curve, with the conditions that these intersections are the closest to the vertical axis, and the adjacent second-order derivatives have similar frequencies. x is a second-order derivative which is within the range of a to b. $P(x)$ is the frequency of x in the image, i.e., the height of the interval at x. $H(x)$ is the height of the curve at the location that corresponds to x.

For an SEM image with low noise, the middle region of the second-order histogram extends above the curve, as can be seen in Figure 2. In this case, it considers ΔA to be zero.

The ratio of ΔA to the total number of pixels N in the image increases as the noise increases. The step uses the ratio to calculate the factor ϕ in Equation (3). In turn, the step uses the equation to estimate the target standard deviation σ_{trgt} via Equation (4). The development of Equations (2) to (4) used tests with the images with additive noise.

$$\phi = \left(1 - \frac{\Delta A}{N}\right)^{\left(1+\frac{\Delta A}{N}\right)\left(1-\frac{\Delta A}{N}\right)} \tag{3}$$

$$\sigma_{trgt} = \left(1 - \frac{\Delta A}{N}\right)\left(1 + \frac{\Delta A}{N}\right)\sigma^{\phi} \tag{4}$$

σ is the standard deviation of the distribution of second-order derivatives in the noisy image.

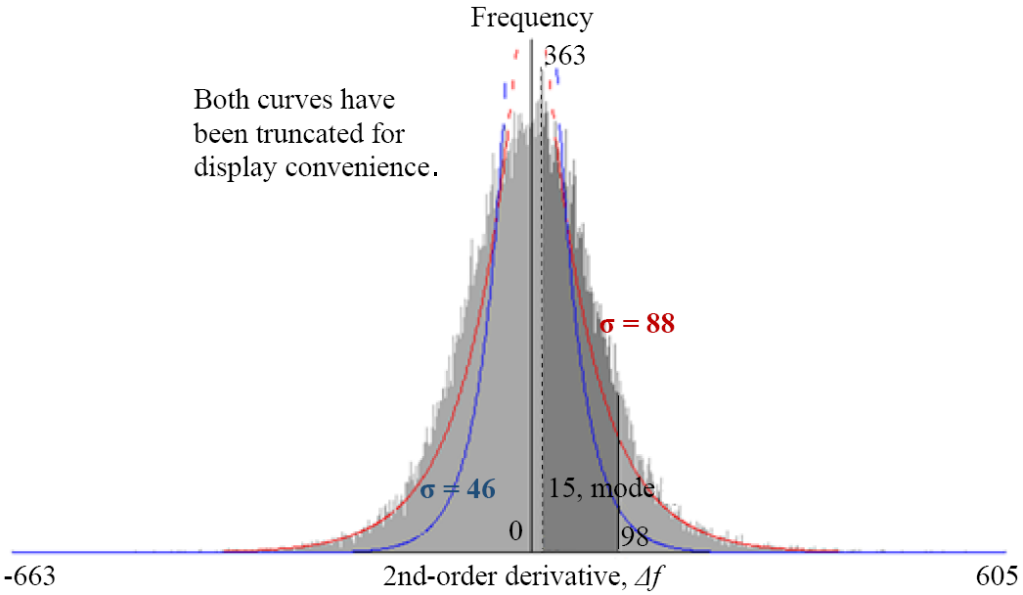

FIGURE 4. Second-order histogram with an additional Laplace curve of $\sigma = 46$ and the interval (shaded darker) where a pixel is to be reallocated

Step 3.2. Imposition of additional Laplace curve. This step creates an additional curve, as shown in Figure 4, with the target standard deviation from the previous step.

Step 3.3. Maximum extent of change and determination of the range of searching for pixels to be reallocated. In the methodology, the second-order derivative of a currently evaluated pixel is changed to a specific value, which is lower than its original is. Yet, there is risk of excessive blurring if the change is too great. To mitigate excessive blurring, there has to be a maximum to the extent of change. Two ranges of second-order derivatives represent this maximum extent. The step searches and selects pixels for changing within these ranges. It does not select any pixels with derivatives that lie outside these ranges.

The step uses one of the ranges for searching the pixels that reside in the negative side of the second-order histogram, while the other range is for the pixels that are in the positive side. The hypothesis is that this accounts for image details that cause the second-order histogram to be not symmetrical about the vertical axis, such as secondary electron emissions.

One of the factors for the ranges is the difference between the extreme ends of the second-order histogram and the ends of the second Laplace curve. The step incorporates this into Equations (5) and (6). Equation (7) determines the factor ψ.

$$\Delta d_{\text{positive}} = \frac{\left|(\nabla^2 f)_{\text{max, histogram}} - (\nabla^2 f)_{\text{max, 2nd curve}}\right|}{\psi} \tag{5}$$

$$\Delta d_{\text{negative}} = \frac{\left|(\nabla^2 f)_{\text{min, histogram}} - (\nabla^2 f)_{\text{min, 2nd curve}}\right|}{\psi} \tag{6}$$

where $\Delta d_{\text{positive}}$ is the extent of the range of searching for pixels on the positive side of the histogram. $\Delta d_{\text{negative}}$ is the range extent for the negative side. $(\nabla^2 f)_{\text{max, histogram}}$ is the highest positive second-order derivative in the histogram. $(\nabla^2 f)_{\text{min, histogram}}$ is the lowest negative second-order derivative. $(\nabla^2 f)_{\text{max, 2nd curve}}$ is the second-order derivative that corresponds to the right end of the second Laplace curve, on the positive side of the

histogram. $(\nabla^2 f)_{\min,\,2\text{nd curve}}$ is the second-order derivative that corresponds to the left end of the second Laplace curve, on the negative side of the histogram.

$$\psi = \begin{cases} 32, & \text{if } \sigma < 1.1\sigma_{trgt} \\ 32 - 80\left(\left(\frac{\sigma}{\sigma_{trgt}} - 1\right)\right), & \text{if } 1.1\,\sigma_{trgt} < \sigma < 1.3\sigma_{trgt} \\ 8 - 20\left(\left(\frac{\sigma}{\sigma_{trgt}} - 1.3\right)\right), & \text{if } 1.3\sigma_{trgt} < \sigma < 1.45\sigma_{trgt} \\ 5 - \left(\frac{\sigma}{\sigma_{trgt}} - 1.45\right), & \text{if } 1.45\sigma_{trgt} < \sigma < 1.9\sigma_{trgt} \\ 4.45 - (1.45)^{\frac{\sigma}{\sigma_{trgt}} - 1.1}, & \text{if } 1.9\sigma_{trgt} < \sigma < 2.3\sigma_{trgt} \\ 1.5, & \text{if } 2.3\sigma_{trgt} < \sigma < 2.85\sigma_{trgt} \\ 1, & \text{if } \sigma > 2.85\sigma_{trgt} \end{cases} \tag{7}$$

where ψ is the factor used in Equations (5) and (6). σ and σ_{trgt} are in Equations (3) and (4).

The piece-wise equations, different conditions and values for the factor ψ in Equation (7) were developed through tests with the 330 sample images with additive noise. The subsequent conditions and corresponding piece-wise equations after the first are used for images with increasing levels of noise, as indicated by the increasingly greater ratio of σ to σ_{trgt}. The equations and values in the conditions provide appreciable changes from one iteration to the next as the images are processed. They prevent excessive blurring across varying levels of noise in the sample images with additive noise.

Step 3.4. Selection of second-order derivatives under target frequencies. This step changes the profile of the second-order histogram such that it approaches the second imposed Laplace curve, as described in Step 3.2. To do so, the second-order derivatives with frequencies that do not reach the curve are to have their frequencies increased. Among these second-order derivatives, the step selects the smallest in magnitude, i.e., the one closest to the vertical axis of the second-order histogram, before the others in order of increasing magnitude as the steps reiterate. The step passes the selection to Step 3.5.

Step 3.5. Determination of the range of second-order derivatives to search for eligible pixels. To increase the frequency of the selected second-order derivative in Step 3.4, pixels with second-order derivatives in its vicinity have their derivative value changed to the value of the selected derivative. The extent of the aforementioned vicinity is not more than the magnitudes of the Δd values that have been determined in Step 3.3. If the selected derivative is negative, the range extent $\Delta d_{\text{negative}}$ is used. If it is positive, $\Delta d_{\text{positive}}$ is used. If the selected derivative is zero, this step uses half of $\Delta d_{\text{negative}}$ for the search in the negative side and half of $\Delta d_{\text{positive}}$ for the positive side. After the step establishes the searching range, it marks the pixels with second-order values within the range so as to subject them to the next step.

Figure 4 shows an example for the results of the procedures from Step 3.3 to Step 3.5. In this example, Step 3.4 selected the second-order derivative of 15, which is a second-order derivative on the positive side of the second-order histogram. Therefore, the relevant range extent is $\Delta d_{\text{positive}}$, which Step 3.3 calculated to be 83. Thus, this step searches the range of second-order derivatives from 16 to 98 (inclusive of 98) for eligible pixels, as highlighted with a darker shade of gray in Figure 4.

Step 3.6. Utilization of the differences in second-order derivatives of neighbouring pixels for the selection process. Neighbouring pixels that are part of the same image detail, such as the edge of an object, have similar second-order derivatives. Figure 1(c) shows this. This step uses this to mitigate blurring in a way that is similar

to the use of local minima and maxima intensities in identifying regions for exposure enhancement [13].

For each of the pixels passed from the previous step, ranges of values are determined from the derivatives of the currently evaluated pixel and its neighbours. Equation (8) expresses the extent of each range:

$$\Delta\left(\nabla^2 f\right) = \frac{(\nabla^2 f)_{\max} - (\nabla^2 f)_{\min}}{n} \tag{8}$$

where $\Delta(\nabla^2 f)$ is the extent of each range. $(\nabla^2 f)_{\max}$ is the highest second-order derivative among the currently evaluated pixel and its neighbours; this is usually a positive value. $(\nabla^2 f)_{\min}$ is the lowest derivative among the pixels; this is usually a negative value. n is the number of pixels, inclusive of the currently evaluated pixel and its neighbours.

The first of the ranges is $(\nabla^2 f)_{\min}$ to $(\nabla^2 f)_{\min} + \Delta(\nabla^2 f)$, and the last is $(\nabla^2 f)_{\max} - \Delta(\nabla^2 f)$ to $(\nabla^2 f)_{\max}$. Thus, there are as many ranges as there are neighbours around the currently evaluated pixel. The grouping of the pixel and its neighbours is according to these ranges. This is similar to the labelling and grouping of pixel values in connected-component labelling techniques [16], except that this uses the second-order derivatives of the pixels instead of their intensity values.

If the currently evaluated pixel happens to populate a range on its own, the pixel advances to the next step. Otherwise, this step repeats with the next pixel in the sequence of selection as established in Step 3.5.

Step 3.7. Changing the second-order derivatives of selected pixels and their neighbours. Each of the pixels from Step 3.6 has its second-order derivative changed to the value that Step 3.4 determined. To achieve this, this step changes the gray value of the pixel such that its second-order derivative, when recalculated, is equal to the target value. The target value is always lower than the initial second-order value of the pixel, due to the conditions of Step 3.4. This resulted in a better balance of detail preservation and noise mitigation than the use of the averages or medians of gray values.

The second-order values of the neighbor pixels are re-calculated. The processing of any subsequent pixels in the image uses these re-calculated values.

Step 3.8. Iterations and termination conditions. This step repeats the procedures in Steps 3.6 and 3.7 on every pixel that has been marked in Step 3.5. A single iteration of this process produces changes that are too small for a noticeable result. Therefore, this step repeats the procedures from Step 3.5 to Step 3.7 iteratively until they achieve the termination conditions. Steps 3.3 to 3.6 establish the termination conditions. The main termination condition is that it is the achievement or surpassing of the target frequency. The second condition is that none of the pixels within the range of searching satisfies the conditions in Step 3.6. The third condition is that despite the selection and processing of pixels, there were no effective changes.

This step repeats Step 3.4 in order to select another second-order derivative value that is under its target frequency. The steps after Step 3.4 repeat, until they have accounted for all of the second-order derivative values that have frequencies below their targets. The number of iterations depends on the range extents and the target frequency as defined in Steps 3.3 and 3.4 respectively. In other words, noisier images, which cause greater range extents and higher target frequencies, require more iterations.

Step 3.9. Comparison with Gaussian blur filter, alpha-trimmed filter & hybrid mean filter. Image filter research has used the Gaussian blur filter for its effect on high levels of noise [17], the alpha-trimmed filter for its effect on non-Gaussian noise [18] and the hybrid median filter for impulse noise [19]. Incidentally, SEM images can have these

noise conditions. Thus, there is the comparison of the proposed method with these filters. Scripts from LIBROW.com form the basis for the filters that are used for this comparison. The default settings for the scripts are such that the Gaussian blur has a window size of 5 and the alpha-trimmed filter has an alpha parameter of 6.

4. **Results and Discussion.** Figure 5 shows an example of the application of the filter on an SEM image with additive noise. Figure 6 shows the second-order histograms of the images in Figure 5.

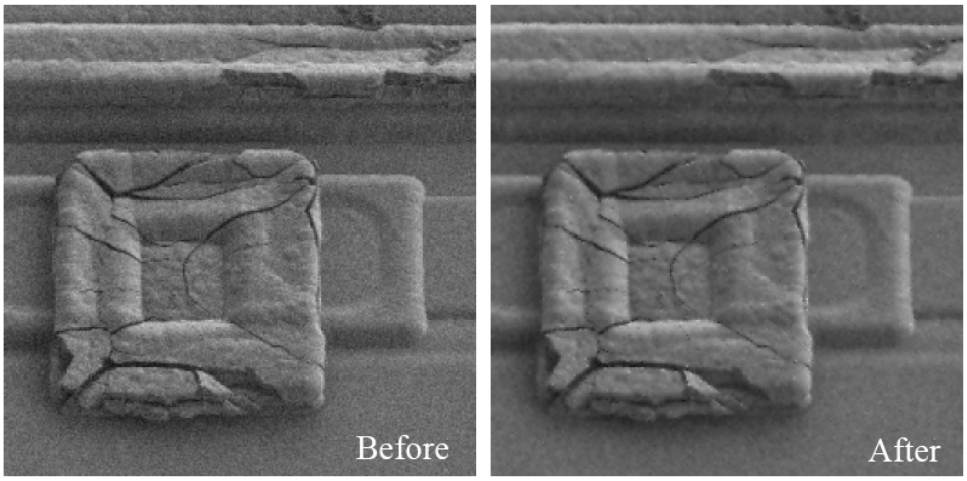

FIGURE 5. Side-by-side comparison of the results of filtering the SEM image in Figure 1(a) with additive Gaussian noise of standard deviation of 8

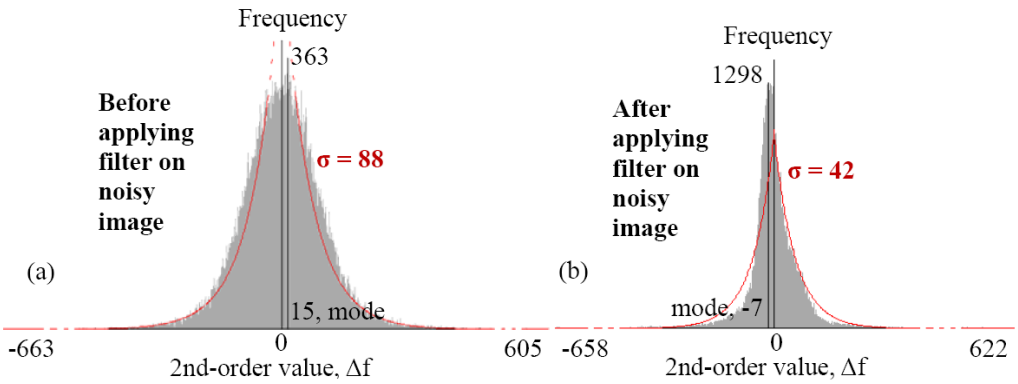

FIGURE 6. Side-by-side comparison of histograms for the SEM images in Figure 5

4.1. **Results of testing on SEM images with additive noise.** The averaged results of applying the filter across the 30 samples of SEM images with additive noise are in Table 1. (There are more levels of additive noise used in the tests than shown in the table; the levels in the table are selected for the most noticeable differences in the results.) The effectiveness of the filter at reducing noise decreases as the noise level increases. This also occurs in the SEM images with different machine conditions, wherever there are high levels of noise.

Explanation: Noise increases the second-order derivatives of affected pixels, thus expanding the range of the second-order histogram of the image and moving pixels away

TABLE 1. Averaged results across 30 sample images with introduced additive noise

Nominal standard deviation of distribution of additive noise in images	Before application of filter		After application of filter	
	Averaged PSNR	Averaged SSIM	Averaged PSNR	Averaged SSIM
2	41.23	0.9983	39.91	0.9978
5	33.90	0.9923	34.15	0.9931
10	27.97	0.9707	29.67	0.9815
15	24.48	0.9374	27.26	0.9678
20	22.03	0.8962	25.13	0.9473

from the middle of the histogram, i.e., flattening it. Figure 6(a) shows this. The proposed method reallocates selected pixels to move them towards the center. This also reduces the range of second-order derivatives, i.e., restoring the profile of the histogram. As a result, there are less pixels with noise in the image generated from the changed data. However, as the proposed method is conservative in its selection of pixels in order to mitigate excessive blurring, it is not effective at high levels of noise, where considerable blurring would be needed to reduce the differences in values between pixels.

4.2. **Hypothesis testing.** The hypothesis is that the proposed method reduces noise in SEM images. The testing of the hypothesis uses SEM images with introduced additive noise. The standard deviation of the noise distribution represents the severity of the additive noise, before and after filtering the image. Table 2 shows the results. Like Table 1, the tests used more levels of noise than shown; the noise levels in the table are selected for the most noticeable differences in the results. They indicate that the filtering method causes near-negligible blurring at low levels of noise.

TABLE 2. Standard deviations of the additive noise across 30 sample images with introduced additive noise, before and after application of the filter

Nominal standard deviation of additive noise	Averaged actual standard deviation of additive noise	
	Before application of filter	After application of filter
2	2.48	2.83
4	4.32	4.27
8	8.19	7.23
10	10.20	8.30
15	15.14	10.87
20	20.01	13.63

Explanation: Due to the conservative selection of pixels, the proposed method does better at low levels of noise than it does at high levels of noise. At low levels of noise, it is capable of avoiding the blurring of edges and picking out the few number of pixels that are affected by noise.

4.3. **Observations on ψ factor.** The piece-wise function in Equation (7) is developed through comparing the changes in the PSNR and SSIM of the resulting image after changing the value of ψ and its associated conditions. Currently, it is composed of a

significant piece-wise equation with several conditions, but it makes a correlation between the standard deviation of the second-order derivative values and the maximum change that can be applied on the second-order values of pixels without causing excessive blurring.

Explanation: As mentioned earlier, Step 3.3 introduces the multiple conditions into Equation (7) to improve the response of the proposed method to varying levels of noise. They are not arbitrary, because they have been developed through considerable testing with the 30 sample images and their 300 noise-added variants and they follow a decreasing trend in order to extend the range of pixel selection at higher levels of noise.

4.4. **Use of iterations.** There are multiple consecutive iterations of the filtering process to compound the changes by a previous iteration onto the next one. This is necessary for any noticeable change in the image to occur at the end. This is similar to the use of iterations to compensate for the low amplification factors in the insertion of watermarks in images [20]. However, as the noise level increases, there have to be more iterations as there are more pixels to search and process.

Explanation: The range of selected second-order derivatives, as described in Step 3.5, increases as the noise level increases. Furthermore, since noise flattens the second-order histogram of an image, there are more pixels across the range of second-order derivatives. This in turn increases the number of iterations to search for eligible pixels.

4.5. **Results of comparison with Gaussian blur, alpha-trimmed and hybrid median filters.** The other filters reduce the contrast of the images more than the proposed method does at any level of noise. However, the proposed method performs poorer than the other methods at high levels of noise. Table 3 shows an example of the comparisons of the proposed method to different filters.

If the machine conditions result in images with clear edges and region boundaries, the proposed method preserves these better than the other filters. The results for an SEM image of leaf cells with different chamber pressures in Table 4 show this. Figure 7 shows the resulting image produced by the proposed method.

TABLE 3. Results of application of the proposed method, Gaussian blur, alpha-trimmed and hybrid median filters on the noise-added variants of the SEM image in Figure 1

σ	After application of the proposed method			After application of Gaussian blur filter		
	PSNR	SSIM	RMSC	PSNR	SSIM	RMSC
2	40.5	0.997	0.1041	33.6	0.986	0.0990
6	32.9	0.985	0.1026	32.4	0.982	0.0994
10	29.9	0.971	0.1008	30.6	0.973	0.1003
20	25.5	0.924	0.1041	26.7	0.937	0.1045
σ	After application of hybrid median filter			After application of alpha-trimmed filter		
	PSNR	SSIM	RMSC	PSNR	SSIM	RMSC
2	35.7	0.992	0.1016	31.7	0.979	0.0992
6	32.5	0.983	0.1021	30.9	0.975	0.0993
10	29.6	0.967	0.1033	29.7	0.967	0.0997
20	24.7	0.905	0.1097	26.7	0.935	0.1025

σ, nominal standard deviation of additive noise distribution in image

TABLE 4. Results of application of filters on SEM images with different chamber pressures; chamber pressure of 10 Pa used as ground truth

Chamber pressure	50 Pa			100 Pa			200 Pa		
	PSNR	SSIM	RMSC	PSNR	SSIM	RMSC	PSNR	SSIM	RMSC
Proposed method	22.5	0.699	0.0700	21.6	0.661	0.0790	20.7	0.654	0.0604
Gaussian blur filter	22.4	0.682	0.0667	21.8	0.673	0.0742	20.5	0.648	0.0583
Hybrid median filter	22.4	0.690	0.0429	21.6	0.664	0.0353	20.5	0.646	0.0512
Alpha-trimmed filter	22.3	0.673	0.0658	21.8	0.668	0.0726	20.5	0.640	0.0566

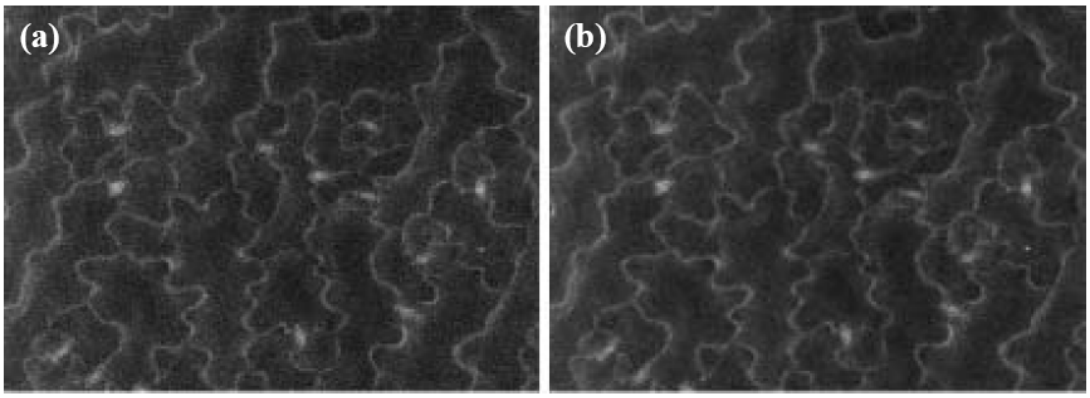

FIGURE 7. Results of filtering an SEM image of leaf cells with a chamber pressure of 200 Pa: (a) unfiltered image, (b) proposed method. Image source for (a): Talbot & White.

Explanation: The other methods do not have the operations as described in Steps 3.3 to 3.5. These steps provide filtering that is more conservative than the other methods, in order to prevent excessive blurring and loss of contrast. Consequently, at high levels, it changes fewer pixels than the other methods do, thus leading to lesser performance at high levels of noise.

5. **Conclusions.** The proposed method shows that the utilization of a histogram of second-order derivatives for the selection of pixels for filtering is feasible at preserving the edges of objects, especially in images with low levels of noise. However, the proposed method is less effective when used on heavily corrupted images.

5.1. **Future direction.** The performance of the proposed method at higher levels of noise is to be improved. One idea is to reduce the conservativeness of the pixel selection in Step 3.6 by introducing more criteria and exceptions that apply to higher levels of noise. Another alternative idea would use the histograms of second-order derivatives as an additional factor for established filter methods, i.e., replacing Steps 3.6 to 3.8 with the techniques used in the other filters.

5.2. **Further research ideas.** The current version of the method does not preserve fine texture details such as surfaces with relatively minor roughness as observed under an SEM. With refinements to the stage of pixel selection, the method is expected to be able to differentiate between pixels that form such details and pixels that are affected by noise. One idea is to implement an algorithm that is more complex than Equation (8) in order to produce ranges with dissimilar extents, thus easing the determination of pixels that have significantly different second-order derivative values compared to their neighbours. Equations (4) to (7) can be developed further so that less iterations are needed.

REFERENCES

[1] R. Rani and S. Kumari, An approach of detecting discontinuities in images, *International Journal of Science and Research (IJSR)*, vol.5, no.7, pp.745-753, 2016.

[2] Y. Wan, T. Lu, W. Yang and W. Huang, A novel image segmentation algorithm via neighborhood principal component analysis and Laplace operator, *International Conference on Network and Information Systems for Computers (ICNISC)*, 2015.

[3] H. Kaur and N. Sohi, A study for applications of histogram in image enhancement, *The International Journal of Engineering and Science (IJES)*, vol.6, no.6, pp.59-63, 2017.

[4] L. Y. Zhuang and Y. P. Guan, Image enhancement via sub image histogram equalization based on mean and variance, *Computational Intelligence and Neuroscience*, 2017.

[5] R. Celestre, M. Rosenberger and G. Notni, A novel algorithm for bad pixel detection and correction to improve quality and stability of geometric measurements, *Journal of Physics: Conference Series*, no.772, 2016.

[6] S. Kaur and R. Singh, Image de-noising techniques: A review paper, *International Journal for Technological Research in Engineering*, vol.2, no.8, 2015.

[7] R. C. Gonzalez and R. E. Woods, *Digital Image Processing*, 2nd Edition, Prentice-Hall, NJ, 2002.

[8] C. J. R. Sheppard and C. J. Cogswell, Signal strength and noise in confocal microscopy: Factors influencing selection of an optimum detector aperture, *Scanning*, vol.13, no.3, pp.233-240, 1991.

[9] K. S. Sim, M. A. Kiani, M. E. Nia and C. P. Tso, Signal-to-noise ratio estimation on SEM images using cubic spline interpolation with Savitzky-Golay smoothing, *Journal of Microscopy*, vol.253, no.1, pp.1-11, 2014.

[10] M. J. Talbot and R. G. White, Cell surface and cell outline imaging in plant tissues using the backscattered electron detector in a variable pressure scanning electron microscope, *Plant Methods*, vol.9, no.40, 2013.

[11] D. Salomon, *Data Compression: The Complete Reference*, 4th Edition, Springer, 2007.

[12] Z. Wang, A. C. Bovik, H. R. Sheikh and E. P. Simoncelli, Image quality assessment: From error visibility to structural similarity, *IEEE Trans. Image Progressing*, vol.13, no.4, pp.600-612, 2004.

[13] E. Peli, Contrast in complex images, *Journal of the Optical Society of America A*, vol.7, no.10, pp.2032-2040, 1990.

[14] W. T. Chan and K. S. Sim, Adaptive pixel targeting and filtering with adjacency variations in second-order derivatives of pixel values for SEM images, *International Conference on Robotics, Automation and Sciences (ICORAS)*, no.3, 2016.

[15] K. Singh, R. Kapoor and S. Sinha, Enhancement of low exposure images via recursive histogram equalization algorithms, *International Journal for Light and Electron Optics*, vol.126, no.20, pp.2619-2625, 2015.

[16] E. S. A. Silva and H. Pedrini, Connected-component labeling based on hypercubes for memory constrained scenarios, *Expert Systems with Applications*, vol.61, pp.272-281, 2016.

[17] E. S. Gedraite and M. Hadad, Investigation on the effect of a Gaussian blur in image filtering and segmentation, *International Symposium Electronics in Marine (ELMAR)*, 2011.

[18] R. Oten and R. J. P. Figueiredo, Adaptive alpha-trimmed mean filters under deviations from assumed noise model, *IEEE Trans. Image Processing*, vol.13, no.5, pp.627-639, 2004.

[19] M. R. Rakesh, B. Ajeya and A. R. Mohan, Hybrid median filter for impulse noise removal of an image in image restoration, *International Journal of Advanced Research in Electrical, Electronics and Instrumentation Engineering*, vol.2, no.10, 2013.

[20] R. K. Jha and R. Chouhan, Dynamic stochastic resonance-based grayscale logo extraction in hybrid SVD-DCT domain, *Journal of the Franklin Institute*, vol.351, no.5, pp.2938-2965, 2014.

Appendix A: Flow Chart of Program.

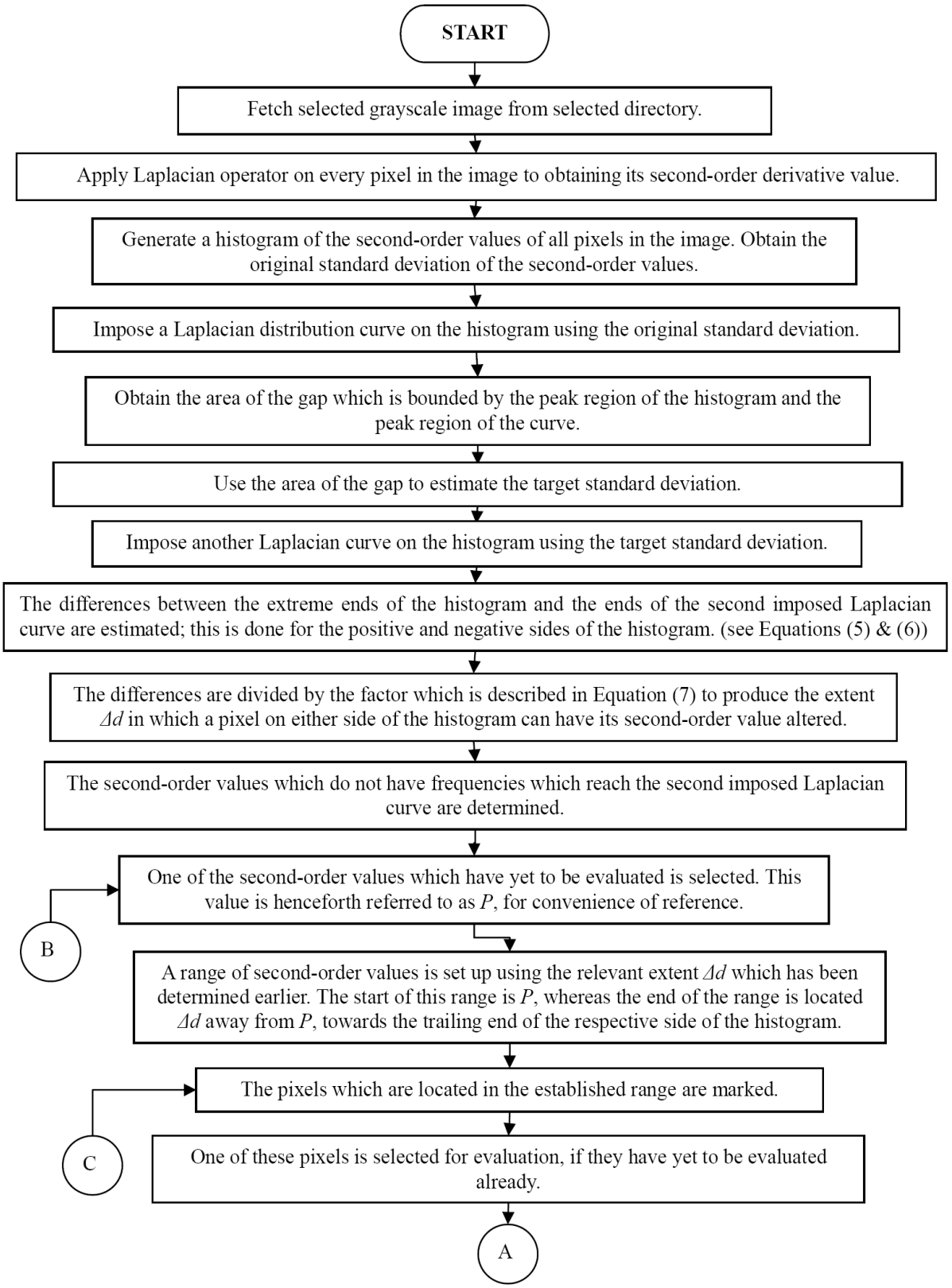

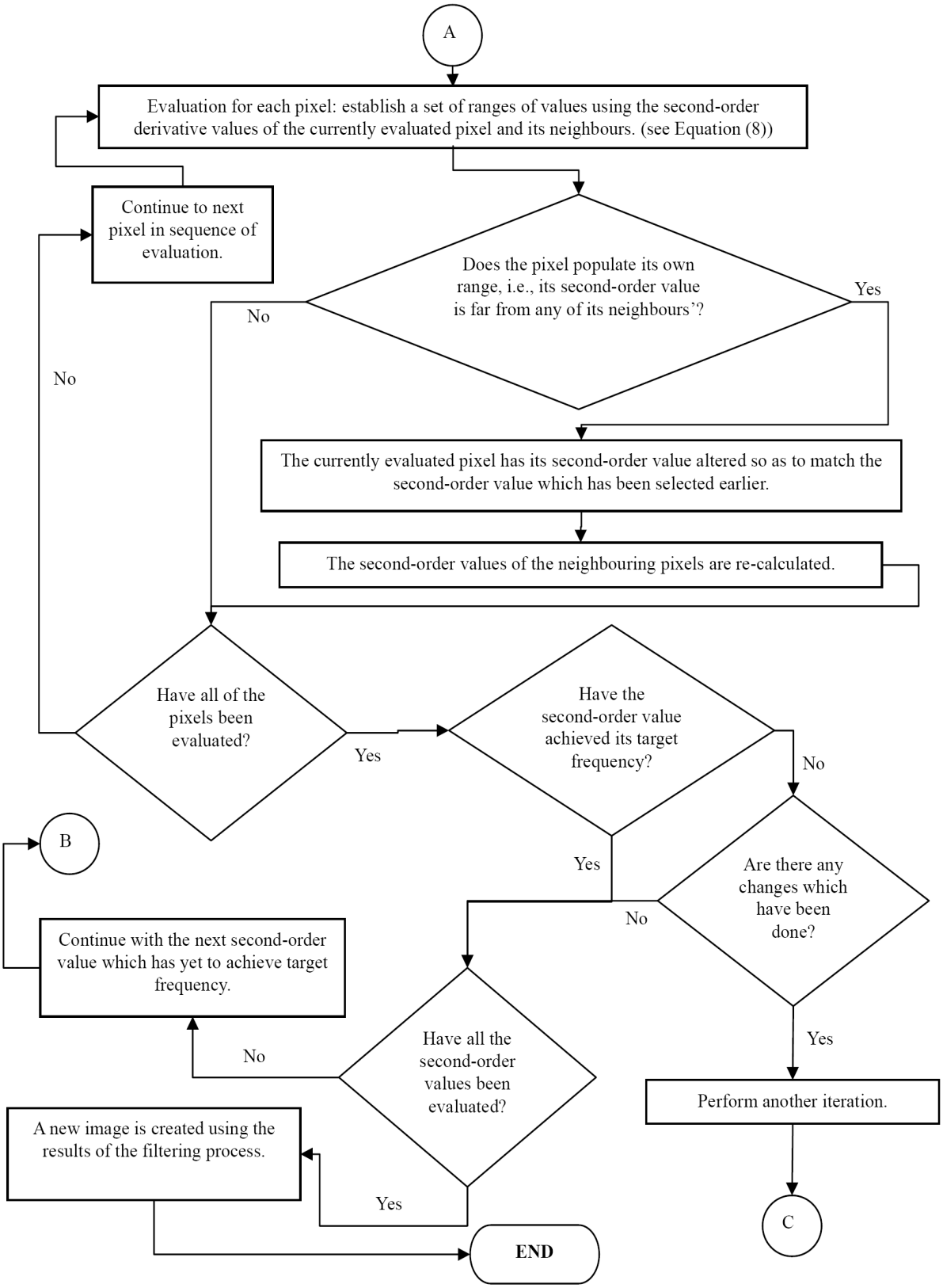
A
Evaluation for each pixel: establish a set of ranges of values using the second-order derivative values of the currently evaluated pixel and its neighbours. (see Equation (8))
Continue to next pixel in sequence of evaluation.
Does the pixel populate its own range, i.e., its second-order value is far from any of its neighbours'?
Yes
No
No
The currently evaluated pixel has its second-order value altered so as to match the second-order value which has been selected earlier.
The second-order values of the neighbouring pixels are re-calculated.
Have all of the pixels been evaluated?
Yes
Have the second-order value achieved its target frequency?
No
B
Yes
Are there any changes which have been done?
No
Continue with the next second-order value which has yet to achieve target frequency.
Have all the second-order values been evaluated?
No
Yes
Perform another iteration.
A new image is created using the results of the filtering process.
Yes
C
END